Available online at www.sciencedirect.com

ScienceDirect

Nuclear and Particle Physics Proceedings 273–275 (2016) 1876–1882

www.elsevier.com/locate/nppp

Search of Neutrinoless Double Beta Decay with the GERDA Experiment

M. Agostini[n], M. Allardt[c], A. M. Bakalyarov[l], M. Balata[a], I. Barabanov[j], L. Baudis[r], C. Bauer[f], N. Becerici-Schmidt[m], E. Bellotti[g,h], S. Belogurov[k,j], S. T. Belyaev[l], G. Benato[r,*], A. Bettini[o,p], L. Bezrukov[j], T. Bode[n], D. Borowicz[b], V. Brudanin[d], R. Brugnera[o,p], D. Budjáš[n], A. Caldwell[m], C. Cattadori[h], A. Chernogorov[k], V. D'Andrea[a], E. V. Demidova[k], A. Domula[c], E. Doroshkevich[j], V. Egorov[d], R. Falkenstein[q], O. Fedorova[j], K. Freund[q], N. Frodyma[b], A. Gangapshev[j,f], A. Garfagnini[o,p], C. Gooch[m], C. Gotti[g,h], P. Grabmayr[q], V. Gurentsov[j], K. Gusev[l,d], W. Hampel[f], A. Hegai[q], M. Heisel[f], S. Hemmer[o,p], G. Heusser[f], W. Hoffmann[f], M. Hult[e], L. V. Inzhechik[j], L. Ioannucci[a], J. Janicksó Csáthy[n], J. Jochum[q], M. Junker[a], V. Kazalov[j], T. Kihm[f], I. V. Kirpichnikov[k], A. Kirsch[f], A. Klimenko[f,d], K. T. Knöpfle[f], O. Kochetov[d], V. N. Kornoukhov[k,j], V. V. Kuzminov[j], M. Laubenstein[a], A. Lazzaro[n], V. I. Lebedev[l], B. Lehnert[c], H. Y. Liao[m], M. Lindner[f], I. Lippi[p], A. Lubashevskiy[f], B. Lubsandorzhiev[j], G. Lutter[e], C. Macolino[a], B. Majorovits[m], W. Maneschg[f], G. Marissens[e], E. Medinaceli[o,p], M. Misiaszek[b], P. Moseev[j], I. Nemchenok[d], S. Nisi[a], D. Palioselitis[m], K. Panas[b], L. Pandola[a], K. Pelczar[b], G. Pessina[h], A. Pullia[i], M. Reissfelder[f], S. Riboldi[i], N. Rumyantseva[d], C. Sada[o,p], M. Salathe[f], C. Schmitt[q], B. Schneider[c], J. Schreiner[f], O. Schulz[m], B. Schwingenheuer[f], S. Schönert[n], H. Seitz[m], O. Selivalenko[j], E. Shevchik[d], M. Shirchenko[l,d], H. Simgen[f], A. Smolnikov[f], L. Stanco[p], M. Stepaniuk[f], H. Strecker[f], C. A. Ur[p], L. Vanhoefer[m], A. A. Vasenko[k], A. Veresnikova[j], K. von Sturm[o,p], V. Wagner[f], M. Walter[r], A. Wegmann[f], T. Wester[c], C. Wiesinger[n], H. Wilsenach[c], M. Wojcik[b], E. Yanovich[j], P. Zavarise[a], I. Zhitnikov[d], S. V. Zhukov[l], D. Zinatulina[d], K. Zuber[c], G. Zuzel[b]

[a] *INFN Laboratori Nazionali del Gran Sasso, LNGS, Assergi, Italy*
[b] *Institute of Physics, Jagiellonian University, Cracow, Poland*
[c] *Institut für Kern- und Teilchenphysik, Technische Universität Dresden, Dresden, Germany*
[d] *Joint Institute for Nuclear Research, Dubna, Russia*
[e] *Institute for Reference Materials and Measurements, Geel, Belgium*
[f] *Max-Planck-Institut für Kernphysik, Heidelberg, Germany*
[g] *Dipartimento di Fisica, Università Milano Bicocca, Milano, Italy*
[h] *INFN Milano Bicocca, Milano, Italy*
[i] *Dipartimento di Fisica, Università degli Studi di Milano e INFN Milano, Milano, Italy*
[j] *Institute for Nuclear Research of the Russian Academy of Science, Moscow, Russia*
[k] *Institute for Theoretical and Experimental Physics, Moscow, Russia*
[l] *National Research Center "Kurchatov Institute", Moscow, Russia*
[m] *Max-Plank-Institut für Physik, München, Germany*
[n] *Physik Department and Excellence Cluster Universe, Technische Universität München, Germany*
[o] *Dipartimento di Fisica e Astronomia dell'Università di Padova, Padova, Italy*
[p] *INFN Padova, Padova, Italy*
[q] *Physikalisches Institut, Eberhard Karls Universität Tübingen, Tübingen, Germany*
[r] *Physik Institut der Universität Zürich, Zürich, Switzerland*

Abstract

The GERDA (GERmanium Detector Array) is an experiment for the search of neutrinoless double beta decay ($0\nu\beta\beta$) in ^{76}Ge, located at Laboratori Nazionali del Gran Sasso of INFN (Italy). In the first phase of the experiment, a 90% confidence level (C.L.) sensitivity of $2.4 \cdot 10^{25}$ yr on the $0\nu\beta\beta$ decay half-life was achieved with a 21.6 kg·yr exposure and an unprecedented background index in the region of interest of 10^{-2} counts/(keV·kg·yr). No excess of signal events was found, and an experimental lower limit on the half-life of $2.1 \cdot 10^{25}$ yr (90% C.L.) was established. Correspondingly, the limit on the effective Majorana neutrino mass is $m_{ee} < 0.2$-0.4 eV, depending on the considered nuclear matrix element. The previous claim for evidence of a $0\nu\beta\beta$ decay signal is strongly disfavored, and the field of research is open again.

Keywords: neutrinoless double beta decay, $T^{0\nu}_{1/2}$, ^{76}Ge, enriched Ge detectors

http://dx.doi.org/10.1016/j.nuclphysbps.2015.09.303

1. Introduction

The search for neutrinoless double beta decay is boosted by the discovery of neutrinos oscillation, which is only possible if neutrinos have non-zero mass and if the lepton number conservation is violated by two units. The observation of $0\nu\beta\beta$ decay would enlighten the possible Majorana-nature of neutrinos and provide a measurement of the neutrino mass scale.

The search can be performed with those even-even nuclei for which the β decay is energetically forbidden, but the simultaneous emission of two β particles is not [1]. This two-neutrino double beta decay ($2\nu\beta\beta$) is a Standard Model (SM) process, with half-life in the range of 10^{19}-10^{21} yr. In addition, several extensions of the SM predict the existence of $0\nu\beta\beta$ decay, with only two electrons being emitted. The experimental signature is a continuum from zero to the Q-value ($Q_{\beta\beta}$) of the reaction for the $2\nu\beta\beta$ decay, and a peak at $Q_{\beta\beta}$ for the $0\nu\beta\beta$ mode. The expected decay rate for the $0\nu\beta\beta$ decay with light neutrino exchange is:

$$\left(T^{0\nu}_{1/2}\right)^{-1} = G^{0\nu}(Q_{\beta\beta}, Z) \left|M^{0\nu}\right|^2 \langle m_{ee}\rangle^2 \quad (1)$$

where $G^{0\nu}(Q_{\beta\beta}, Z)$ is the phase space, depending on $Q_{\beta\beta}$ and the nuclear charge Z, $M^{0\nu}$ is the nuclear matrix element, and $\langle m_{ee}\rangle^2 = \left|\sum_{i=1}^{3} U_{ei}^2\, m_i\right|$ is the effective Majorana neutrino mass [2, 3]. The experimental sensitivity for an exclusion limit on the $0\nu\beta\beta$ decay half-life at n_σ C.L. is

$$\hat{T}^{0\nu}_{1/2}(n_\sigma) = \frac{\ln 2 \cdot N_A}{n_\sigma \sqrt{2}} \frac{f_A \cdot \varepsilon}{m_A} \sqrt{\frac{M \cdot t}{BI \cdot \Delta E}} \quad (2)$$

with N_A being the Avogadro number, f_A and m_A the enrichment fraction and the atomic mass of the considered isotope, ε the total efficiency, M the total mass, t the lifetime of the measurement, BI the background index at $Q_{\beta\beta}$ in counts/(keV·kg·yr), and ΔE the energy resolution (full width at half maximum, FWHM) [4].

The presence of several isotope-dependent parameters in Eq. 1 and 2 allows for a great variety of experimental techniques to be exploited in the $0\nu\beta\beta$ decay search. Among the possible choices, ^{76}Ge represents one of the most appealing because of the high total efficiency ($\sim$ 75%) and the possibility of enrichment up to $\sim$ 86%. Even if the ^{76}Ge $Q_{\beta\beta}$ at 2039 keV lies under the end-point of the thorium and radium chain and is therefore in a region where the Compton continuum from these two is the dominant background, the extraordinary energy resolution ($\sim$ 1.5‰ FWHM at $Q_{\beta\beta}$) and the possibility to perform pulse shape discrimination (PSD) enhance the sensitivity and make ^{76}Ge one of the most promising isotopes in the $0\nu\beta\beta$ decay search.

The most recent limits on $T^{0\nu}_{1/2}$ are of order of 10^{25} yr, depending on the isotope. Such a high sensitivity can only be reached if the background level in the region of interest (ROI) is lowered to 10^{-2} – 10^{-3} counts/(keV·kg·yr). Typically this is obtained by locating the experiment underground to reduce the background induced by cosmic radiation, by using active vetoes for the surviving cosmic muons and the external backgrounds, and by minimizing the radioactive contamination of the materials in vicinity of the detectors.

2. The GERDA Experiment

The GERDA experiment consists of a large mass of germanium crystals isotopically enriched to $\sim$ 86% in ^{76}Ge and simultaneously operated as source and detectors for $0\nu\beta\beta$ decay. The detectors are mounted in low-mass copper holders with ultra-low radioactivity and directly immersed in a cryostat filled with 70 ton liquid argon (LAr), acting as cooling medium and shielding from external radiation (see Fig. 1). A 590 m^3 water tank surrounds the LAr cryostat and represents a further shielding from external γ's and neutrons. It is instrumented with 66 PMTs for the detection of Cherenkov light induced by cosmic muons and operated in conjunction with scintillator panels located on the top of the experiment. A detailed description of the experimental setup is provided in [5].

The detectors employed in GERDA are of two types (Fig. 2). The semi-coaxial are characterized by masses of 2-3 kg and an energy resolution (FWHM) at $Q_{\beta\beta}$ of about 2.4‰ achieved in Phase I. The BEGe detectors have masses of about 0.7 kg, a relative FWHM at $Q_{\beta\beta}$ of about 1.6‰, and enhanced PSD capabilities, thanks to the discrimination between $0\nu\beta\beta$ like single site events (SSE) and γ-like multi-site events (MSE) [6, 7]. The use of upgraded signal cables and front-end electronics, together with an optimized signal shaping currently under development, can lead to resolutions of 1.7‰ and 1.2‰ for the coaxial and BEGe detectors, respectively.

A first data collection, denoted as Phase I, has been performed between November 2011 and June 2013 with 8 $^{\text{enr}}$Ge semi-coaxial detectors inherited from the Heidelberg-Moskow (HdM) [8] and IGEX [9] experiments and refurbished at Canberra, Olen [10], and 5

*Corresponding author
Email address: gbenato@physik.uzh.ch (G. Benato)

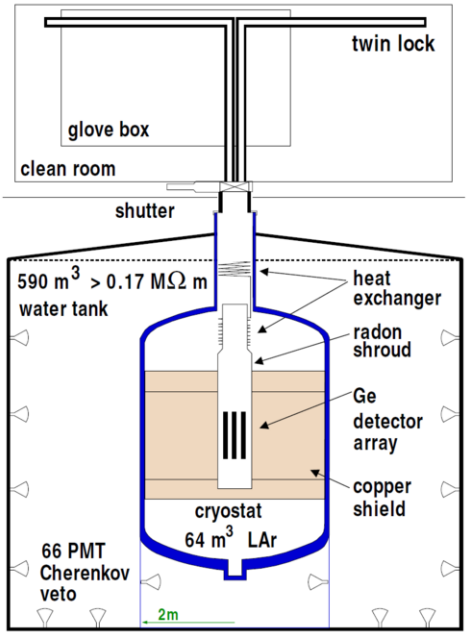

Figure 1: Schematic view of the GERDA setup. The germanium detectors are directly inserted in a 70 ton LAr cryostat, further surrounded by a 590 ton water tank instrumented with PMTs for an active muon veto. A class 7 clean room is present on the top of the structure to minimize the LAr contamination during mounting and maintenance operation.

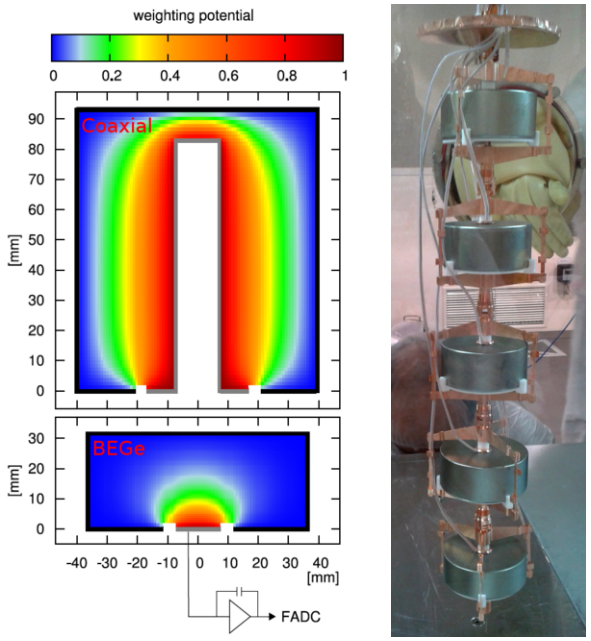

Figure 2: Left: electric potential in semi-coaxial and BEGe detectors. Most of the BEGe volume is characterized by relatively low potential, reflected in longer pulses rise-time and higher discrimination capabilities between SSE and MSE. Right: 5 BEGe detectors being installed in GERDA in July 2012.

Broad Energy Germanium (BEGe) diodes, for a total mass of 17.7 and 3.6 kg, respectively. The high voltage of two of the semi-coaxial detectors had to be set to zero during the data taking due to high leakage current, while the data collected with one of the BEGes were discarded due to frequent gain fluctuations. Thus the total mass considered for the $0\nu\beta\beta$ decay analysis is 17.6 kg, and the total exposure 21.6 kg·yr. This, combined to a BI after PSD of $1.2 \cdot 10^{-2}$ counts/(keV·kg·yr), leads to a median sensitivity of $2.4 \cdot 10^{25}$ yr (see Tab. 1). A second phase is foreseen to start in 2015 with an additional 20 kg mass of BEGe detectors and a BI of one order of magnitude lower. This improved sensitivity is achievable through the installation of PMTs and SiPMs in the LAr for the detection of Ar_2 scintillation light induced by external background radiation from the detector holders and the front-end electronics. Under this condition, a median sensitivity of $(1-2) \cdot 10^{26}$ yr can be achieved with a 100 kg·yr exposure and a live-time of about 3 yr. This will allow to cover a great part of the degenerate neutrino mass region [11].

The data collection is performed via digitization of the charge pulses in the range [60−8000] keV and a subsequent offline analysis with the software tool GELATIO [12]. In GELATIO a set of dedicated quality cuts is in charge of tagging and rejecting events recorded in coincidence among more detectors, as well as pile-ups and events induced by discharges. Finally, the energy estimation is performed with a pseudo-Gaussian shaping.

The energy calibration of Phase I data was performed via (bi)weekly runs with three ^{228}Th sources. The energy resolution at $Q_{\beta\beta}$ is estimated by weighting with the detector exposures and is 4.8 ± 0.2 keV and 3.2 ± 0.2 keV for the semi-coaxial and the BEGe detectors, respectively. The variations in gain between subsequent calibrations are less than 0.05% [5], corresponding to $< 30\%$ of the energy resolution. The stability during the physics runs was monitored with a pulser, injecting charge signals to the preamplifiers input.

During all Phase I data collection, the automatic blinding of the events within a ±20 keV region around $Q_{\beta\beta}$ has been applied with the aim of avoiding any possible bias in the $0\nu\beta\beta$ decay analysis. Neither the number of events, nor their energy and waveforms were available to the collaboration. Once the calibration of the energy spectra and the background model were finalized, a partial unblinding has been performed, leaving a ±5 keV (±4 keV) window still closed for the semi-coaxial (BEGe) detectors. The final unblinding was then performed only once the full chain of data selection, quality cut and analysis procedure had been de-

Table 1: Timeline of the GERDA experiment. The reported mass corresponds to that of ^{76}Ge. The quoted BI is obtained after the PSD application.

	Mass [kg]	BI at $Q_{\beta\beta}$ [counts/(keV·kg·yr)]	Live-time [yr]	Sensitivity to $T^{0\nu}_{1/2}$[yr]	Used detectors
Phase I	15	$\sim 10^{-2}$	1.4	$2.4 \cdot 10^{25}$	6 coaxial, 4 BEGe
Phase II	35	$\sim 10^{-3}$	3-5	$(1\text{-}2) \cdot 10^{26}$	8 coaxial, 30 BEGe

fined and fixed.

3. The Background of GERDA Phase I

The background of GERDA Phase I is fully described in Reference [13]. The energy spectrum obtained with the 6 semi-coaxial and the 4 BEGe detectors used for the construction of the background model is shown in Fig. 3. The low energy region is characterized by a prominent continuum induced by ^{39}Ar β decay (with 565 keV Q-value) in LAr. The dominant contribution between 500 and 1800 keV is represented by the $2\nu\beta\beta$ decay of ^{76}Ge. In addition to this, several γ lines are visible: ^{40}K decay in the detector holders generates a line at 1460 keV, ^{42}K in LAr generates a line at 1525 keV, while the ^{226}Ra and ^{228}Th decay chains are responsible for a few other weaker lines between 1.7 and 2.6 MeV. The background above 4 MeV is dominated by α decays of ^{210}Po and ^{226}Ra contaminants on the detector surface, and is about an order of magnitude higher for the semi-coaxial than for the BEGe detectors.

The background decomposition has been performed on the energy spectrum in the [570; 7500] keV range. For this and for the $0\nu\beta\beta$ decay analysis the data have been divided in datasets, on the basis of the BI and FWHM at $Q_{\beta\beta}$. Hence the data obtained with the semi-coaxial and BEGe detectors are kept separate. Moreover, the data collected with the semi-coaxial detectors have been split in two datasets, denoted as Golden and Silver, with a higher BI in the latter due to the insertion of the BEGes in LAr in July 2012. Two background models have been developed. In the "minimum" model only the known and clearly visible contributions have been considered, while in the "maximum" model more than one possible location for some of the backgrounds are included, too. As an example, in the minimum model ^{42}K is considered to decay in LAr only, while in the maximum model the ^{42}K contributions from the detectors n^+ and p^+ contacts are included, as well. This results in a strong correlation for the weakest parameters, with no clear statement on the favored background origin. Nevertheless, both models agree in the prediction of a flat background in the ROI. The BI at $Q_{\beta\beta}$ obtained from the background models agree with each other, and also with the estimation coming from a spectral fit with a flat distribution in a 200 keV range around $Q_{\beta\beta}$ [13]. Therefore the $0\nu\beta\beta$ decay analysis was performed by simultaneously fitting the spectra relative to the three datasets with a Gaussian distribution over a flat background, with a total of four free parameters ($1/T^{0\nu}_{1/2}$ and the three background levels).

A background suppression of about a factor of 2 is reached thanks to the PSD. For the semi-coaxial detectors, this is performed with an artificial neural network, while for the BEGe the ratio between the height of the current pulse and the event energy is exploited as a discrimination parameter. A detailed report of the two methods and their application is provided in [14]. The choice of the PSD for the two detector types and the relative cuts were defined prior to the final unblinding.

4. Results on $0\nu\beta\beta$ Decay

The unblinding of the side regions around $Q_{\beta\beta}$ revealed no unexpected spectral feature, with an event distribution compatible with a flat background. The final unblinding of the ROI could then be performed, leading to the results reported in Tab. 2. For all the datasets the observed number of counts is compatible with the expectation from the background, estimated through the interpolation with a flat distribution in the [1930; 2160] keV range, excluding the 40 keV blinded region and two 10 keV wide region around the known lines at 2104 and 2119 keV. The same agreement between the experimental values and the expected background is preserved after the application of the PSD. The sum spectrum of the three dataset before and after the PSD use is depicted in Fig. 4.

The fit is performed with the profile likelihood method including the systematic uncertainties due to the detector parameters, the energy scale and resolution, and the efficiency of the quality cuts are folded using a Monte Carlo approach. The correlation between the nuisance parameters is considered as well. The fit is restricted to the physically allowed region $T^{0\nu}_{1/2} > 0$, and it is verified that no under-coverage is present. As a result,

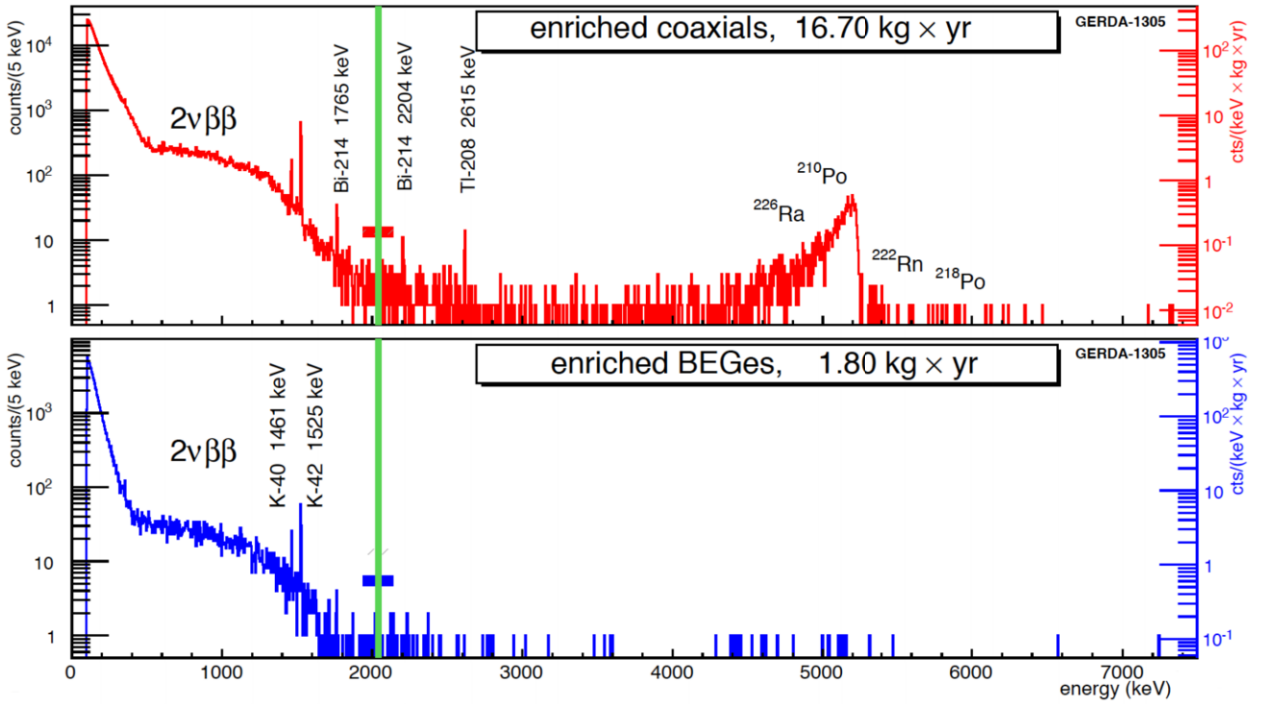

Figure 3: Sum spectra of physics events for the 6 semi-coaxial (top) and the 4 BEGe (bottom) detectors. The green area corresponds to the 40 keV wide blinded region. The most prominent γ lines are labeled, together with the major α contaminants.

no excess of signal counts over the background is found, with a best fit value of $N^{0\nu} = 0$. This is translated to a limit in $T^{0\nu}_{1/2}$ with the formula:

$$T^{0\nu}_{1/2} = \frac{\ln 2 \cdot N_A}{m_A \cdot N^{0\nu}} \cdot f_{76} \cdot f_{av} \cdot \varepsilon_{fep} \cdot \varepsilon_{psd} \cdot m\Delta t \qquad (3)$$

where f_{76} is the ^{76}Ge enrichment fraction, f_{av} the active volume fraction, ε_{fep} the probability for a $0\nu\beta\beta$ decay event to release all its energy in the detector active volume, and ε_{psd} the PSD signal acceptance.

The 90% C.L. limit on the number of signal counts is $N^{0\nu} < 3.5$. Correspondingly, the limit on the $0\nu\beta\beta$ decay half-life is:

$$T^{0\nu}_{1/2} > 2.1 \cdot 10^{25} \text{ yr} \quad (90\% \text{ C.L.}) \qquad (4)$$

which is close to the expected median sensitivity of $2.4 \cdot 10^{25}$ yr. The fit has been performed with a Bayesian method, too, using the Bayesian Analysis Toolkit [15], with a flat prior for $1/T^{0\nu}_{1/2}$ between 0 and 10^{-24} yr^{-1}. Also in this case, a best fit is found for $N^{0\nu} = 0$, and the 90% credibility interval is $T^{0\nu}_{1/2} > 1.9 \cdot 10^{25}$ yr, for a median sensitivity of $2.0 \cdot 10^{25}$ yr. More details regarding the $0\nu\beta\beta$ decay analysis are provided in [16].

The previous claim of $0\nu\beta\beta$ decay evidence [17] with $T^{0\nu}_{1/2} = \left(1.19^{+0.37}_{-0.23}\right) \cdot 10^{25}$ yr is not supported by the present

Table 2: Comparison between the observed number of counts in the ROI and the expectation value from background only for the three datasets before and after the PSD application. All the observed values are consistent with the expected ones within the Poisson uncertainty.

PSD	Dataset	Exposure [kg·yr]	Observed Counts	Expected Background
no	Golden	17.9	5	3.3
	Silver	1.3	1	0.8
	BEGe	2.4	1	1.0
yes	Golden	17.9	2	2.0
	Silver	1.3	1	0.4
	BEGe	2.4	0	0.1

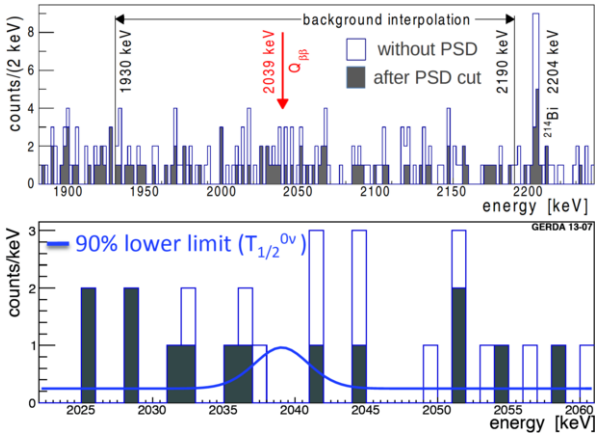

Figure 4: Top: sum spectrum of all the three datasets before and after PSD application. Bottom: detailed view of the spectrum in the 40 keV region around $Q_{\beta\beta}$. The blue line corresponds to the 90% C.L. limit on the signal strength (obtained with a fit on the three dataset separately).

GERDA Phase I result. Assuming the presence of a $0\nu\beta\beta$ decay with a signal strength as quoted in [17], the profile likelihood analysis returns a probability to find a best fit of zero events in the GERDA data equal to 1%. Similarly, a Bayesian comparison of the model including the claimed signal (H_1) and the background-only hypothesis (H_0) provides a Bayes factor $P(N_1)/P(H_0) = 0.024$.

On the contrary, the result presented here is consistent with the limits provided by IGEX in [18] and by a previous result of HdM [19], with $T^{0\nu}_{1/2} > 1.57 \cdot 10^{25}$ yr (90% C.L.) and $T^{0\nu}_{1/2} > 1.9 \cdot 10^{25}$ yr (90% C.L.), respectively. The combination with these yields a best fit for $N^{0\nu} = 0$ and a limit of:

$$T^{0\nu}_{1/2} > 3.0 \cdot 10^{25} \text{ yr} \quad (90\% \text{ C.L.}) \tag{5}$$

with a Bayes factor $P(N_1)/P(H_0) = 2 \cdot 10^{-4}$. Hence the claim reported in [17] is strongly disfavored. Given that only ^{76}Ge based experiments are involved, the comparison presented here is fully model-independent.

The result obtained on $T^{0\nu}_{1/2}$ can be converted to a limit on the effective Majorana neutrino mass by inverting Eq. 1. Using the recently recalculated phase-space factor for ^{76}Ge [20] and the nuclear matrix elements (NME) calculations from [21, 22, 23, 24, 25, 26, 27], we obtain:

$$m_{ee} < 0.2\text{-}0.4 \text{ eV} \tag{6}$$

depending on the considered NME [28]. This result is at the same level with the limits reported by the EXO-200 [29] and KamLAND-Zen [30] Collaborations.

5. Summary

With an exposure of 21.6 kg·yr and a BI of 10^{-3} counts/(keV·kg·yr), GERDA Phase I establishes a limit on $0\nu\beta\beta$ decay half-life corresponding to $T^{0\nu}_{1/2} > 2.1 \cdot 10^{25}$ yr (90% C.L.). The claim for evidence of $0\nu\beta\beta$ decay signal is strongly disfavored with a model-independent measurement. The background reduction by an order of magnitude and the increase of the active mass by about a factor two will allow GERDA Phase II to improve its sensitivity on $T^{0\nu}_{1/2}$ by one order of magnitude, thus covering a great portion of the degenerate neutrino mass region.

References

[1] M. Goeppert Mayer, Double beta-disintegration, Phys. Rev. 48 (1935) 512–516.
[2] W. Rodejohann, Neutrino-less Double Beta Decay and Particle Physics, Int. J. Mod. Phys. E 20 (2011) 1833–1930.
[3] J. J. Gómez-Cadenas et al., The Search for neutrinoless double beta decay, Riv. Nuovo Cim. 35 (2012) 29–98.
[4] F. T. Avignone III et al., Next generation double-beta decay experiments: metrics for their evaluation, New J. Phys. 7 (2005) 6.
[5] M. Agostini et al. (GERDA Collaboration), The GERDA Experiment for the search of $0\nu\beta\beta$ decay in ^{76}Ge, Eur. Phys. J. C 73 (2013) 2330.
[6] D. Budjáš et al., Pulse shape discrimination studies with a Broad-Energy Germanium detector for signal identification and background suppression in the GERDA double beta decay experiment, JINST 4 (2009) P10007.
[7] E. Andreotti et al., HEROICA: an underground facility for the fast screening of germanium detectors, JINST 8 (2013) P06012.
[8] M. Günther et al., Heidelberg-Moskow $\beta\beta$ experiment with ^{76}Ge: Full setup with five detectors, Phys. Rev. D 55 (1997) 54–67.
[9] C. E. Aalseth et al., Recent results from the IGEX double-beta decay experiment, Nucl. Phys. B Proc. Suppl. 48 (1996) 223–225.
[10] Canberra Semiconductios, NV, Lammerdries 25, B-2250, Olen, Belgium.
URL `www.canberra.com`
[11] S. Dell'Oro et al., New expectations and uncertainties on neutrinoless double beta decay, Phys. Rev. D 90 (2014) 033005.
[12] M. Agostini et al., GELATIO: a general framework for modular digital analysis of high-purity Ge detector signals, JINST 6 (2011) P08013.
[13] M. Agostini et al. (GERDA Collaboration), The background of the $0\nu\beta\beta$ experiment GERDA, Eur. Phys. J. C 74 (2014) 2764.
[14] M. Agostini et al. (GERDA Collaboration), Pulse shape discrimination for the GERDA Phase I data, Eur. Phys. J. C 73 (2013) 2583.
[15] A. Caldwell et al., BAT - The Bayesian Analysis Toolkit, Comput. Phys. Commun. 180 (2009) 2197–2209.
[16] M. Agostini et al. (GERDA Collaboration), Results on Neutrinoless Double-β Decay of ^{76}Ge from Phase I of the GERDA Experiment, Phys. Rev. Lett. 111 (2013) 122503.
[17] H. V. Klapdor-Kleingrothaus et al., Search for neutrinoless double beta decay with enriched ^{76}Ge in Gran Sasso 1990 – 2003, Phys. Lett. B 586 (2004) 198–212.

[18] C. E. Aalseth et al. (IGEX Collaboration), IGEX ^{76}Ge neutrinoless double-beta decay experiment: Prospects for next generation experiments, Phys. Rev. D 65 (2002) 092007.
[19] H. V. Klapdor-Kleingrothaus et al., Latest results from the HEIDELBERG-MOSKOW double beta decay experiment, Eur. Phys. J. A 12 (2001) 147–154.
[20] J. Kotila ant F. Iachello, Phase-space factors for double-β decay, Phys. Rev. C 85 (2012) 034316.
[21] T. R. Rodríguez and G. Martínez-Pinedo, Energy Density Functional Study of Nuclear Matrix Elements for Neutrinoless $\beta\beta$ Decay, Phys. Rev. Lett. 105 (2010) 252503.
[22] J. Menéndez et al., Disassembling the nuclear matrix elements of the neutrinoless $\beta\beta$ decay, Nucl. Phys. A 818 (2009) 139–151.
[23] J. Barea et al., Nuclear matrix elements for double-β decay, Phys. Rev. C 87 (2013) 014315.
[24] J. Suhonen ant O. Civitarese, Effects of orbital occupancies and spin-orbit partners on $0\nu\beta\beta$-decay rates, Nucl. Phys. A 847 (2010) 207–232.
[25] A. Meroni et al., Multiple CP Non-conserving Mechanisms of $\beta\beta$-Decay and Nuclei with Largely Different Nuclear Matrix Elements, JHEP 1302 (2013) 25.
[26] F. Šimkovic et al., $0\nu\beta\beta$ and $2\nu\beta\beta$ nuclear matrix elements, quasiparticle random-phase approximation, and isospin symmetry restoration, Phys. Rev. C 87 (2013) 045501.
[27] M. T. Mustonen and J. Engel, Large-scale calculations of the double-β decay of ^{76}Ge, ^{130}Te, ^{136}Xe and ^{150}Nd in the deformed self-consistent Skyrme quasiparticle random-phase approximation, Phys. Rev. C 87 (2013) 064302.
[28] A. Smolnikov and P. Grabmayr, Conversion of experimental half-life to effective electron neutrino mass in $0\nu\beta\beta$ decay, Phys. Rev. C 81 (2010) 028502.
[29] The EXO-200 Collaboration, Search for Majorana neutrinos with the first two years of EXO-200 data, Nature 510 (2014) 229–234.
[30] A. Gando et al. (KamLAND-Zen Collaboration), Limit on Neutrinoless $\beta\beta$ Decay of ^{136}Xe from the First Phase of KamLAND-Zen and Comparison with the Positive Claim in ^{76}Ge, Phys. Rev. Lett. 110 (2013) 062502.